Default mode network connectivity in stable vs progressive mild cognitive impairment

J.R. Petrella, MD
F.C. Sheldon, BS
S.E. Prince, PhD
V.D. Calhoun, PhD
P.M. Doraiswamy, MBBS

Address correspondence and reprint requests to Dr. Jeffrey R. Petrella, Alzheimer Imaging Research Laboratory, Duke University, DUMC-Box 3808, Durham, NC 27710
jeffrey.petrella@duke.edu

ABSTRACT

Objective: Dysfunction of the default mode network (DMN) has been identified in prior cross-sectional fMRI studies of Alzheimer disease (AD) and mild cognitive impairment (MCI); however, no studies have examined its utility in predicting future cognitive decline.

Methods: fMRI scans during a face–name memory task were acquired from a cohort of 68 subjects (25 normal control, 31 MCI, and 12 AD). Subjects with MCI were followed for 2.4 years (±0.8) to determine progression to AD. Maps of DMN connectivity were compared with a template DMN map constructed from elderly normal controls to obtain goodness-of-fit (GOF) indices of DMN expression. Indices were compared between groups and correlated with cognitive decline.

Results: GOF indices were highest in normal controls, intermediate in MCI, and lowest in AD ($p < 0.0001$). In a predictive model (that included baseline GOF indices, age, education, Mini-Mental State Examination score, and an index of DMN gray matter volume), the effect of GOF index on progression from MCI to dementia was significant. In MCI, baseline GOF indices were correlated with change from baseline in functional status (Clinical Dementia Rating–sum of boxes) ($r = -0.40$, $p < 0.04$). However, there was no additional predictive value for DMN connectivity when baseline delayed recall was included in the models.

Conclusions: fMRI connectivity indices distinguish patients with MCI who undergo cognitive decline and conversion to AD from those who remain stable over a 2- to 3-year follow-up period. Our data support the notion of different functional brain connectivity endophenotypes for "early" vs "late" MCI, which are associated with different baseline memory scores and different rates of progression and conversion. *Neurology*® 2011;76:511–517

GLOSSARY

AD = Alzheimer disease; **CDR** = Clinical Dementia Rating; **CDR-SB** = Clinical Dementia Rating–sum of boxes; **CVLT** = California Verbal Learning Test; **DMN** = default mode network; ***DSM-IV*** = *Diagnostic and Statistical Manual of Mental Disorders*, 4th edition; **GIFT** = Group ICA of fMRI Toolbox; **GOF** = goodness-of-fit; **ICA** = independent components analyses; **MCI** = mild cognitive impairment; **MMSE** = Mini-Mental State Examination; **NINCDS-ADRDA** = National Institute of Neurological and Communicative Disorders and Stroke–Alzheimer's Disease and Related Disorders Association; **VBM** = voxel-based morphometry.

Recently, a reciprocal brain network, termed the default mode network (DMN), which becomes less active during engagement in cognitive tasks and more active during periods of rest, has been implicated in the pathophysiology of Alzheimer disease (AD).[1,2] Prior cross-sectional functional neuroimaging studies have shown loss of DMN integrity in AD as well as in mild cognitive impairment (MCI).[3–7] Recent studies of asymptomatic elderly subjects have shown that those with positive amyloid PET scans also demonstrate significant losses in DMN integrity.[5,8,9] The exact relationship between DMN function and future decline is not fully understood, however.

Assessment of brain network connectivity is a relatively new area of focus in fMRI studies, and "connectonomics," the study of the human connectome, has been earmarked as an area of

Editorial, page 498

e-Pub ahead of print on January 12, 2011, at www.neurology.org.

From the Department of Radiology and Brain Imaging and Analysis Center (J.R.P., F.C.S.), Duke Institute of Brain Sciences (J.R.P., S.E.P., P.M.D.), and Departments of Psychiatry and Medicine (P.M.D.), Duke University Medical Center, Durham, NC; and The Mind Research Network & The University of New Mexico (V.D.C.), Albuquerque.

Study funding: Supported by NIH/NIA 1R01AG019728.

Disclosure: Author disclosures are provided at the end of the article.

priority for future neurocognitive research.[10] Functional connectivity is defined as the presence of statistical dependencies, or correlations, among spatially remote neurophysiologic events[11] and several methods have been proposed for measuring it in fMRI research.[12] A notable prior study showed that a quantitative neuroimaging index of DMN connectivity, termed the goodness-of-fit (GOF) index, could distinguish healthy aging from AD cross-sectionally.[4] Instead of using a priori regions of interest, the GOF approach uses a data-driven approach termed independent components analyses (ICA), a technique that decomposes fMRI signals into constituent functional networks, and is particularly effective during complex cognitive tasks where multiple operations occur simultaneously. In this initial prospective, longitudinal study, we examined the utility of GOF indices of functional connectivity in the DMN for predicting cognitive decline in MCI.

METHODS

Standard protocol approvals, registrations, and patient consent. The study was approved by the Duke University Medical Center institutional review board and written informed consent was obtained from all subjects or legal guardian as appropriate.

Subjects. A total of 68 subjects (31 with MCI, 12 with AD, and 25 controls) were included in this study. MCI (amnestic type) subjects had a recent history of symptomatic worsening in memory, impaired delayed recall memory performance, a Clinical Dementia Rating (CDR) global score of 0.5, with 0.5 or greater on the memory score, did not meet National Institute of Neurological and Communicative Disorders and Stroke–Alzheimer's Disease and Related Disorders Association (NINCDS-ADRDA) or *DSM-IV* criteria for dementia, and had normal or near normal independent function. Five subjects with MCI did not have an informant and their diagnostic status was based on neuropsychological tests. Subjects with AD met NINCDS-ADRDA criteria for probable AD. Normal controls had normal cognitive scores and a CDR of 0. All subjects underwent detailed neuropsychiatric examination to exclude confounding significant neuropsychiatric disorders, such as current major depression, as reported previously.[13]

The subjects in this study were selected from a larger cohort (n = 98) and consisted of those who completed an fMRI protocol (3 runs with less than 1 mm of translational motion) and subjects with MCI had at least a 1-year longitudinal follow-up. Subjects with MCI were clinically evaluated every 6 months after baseline until they converted to AD, or until the end of the study period with informant interviews, neuropsychological testing, and CDR ratings. During follow-up, subjects with MCI were reclassified as MCI-converter or MCI-nonconverter based on whether they were subsequently diagnosed with dementia. The clinical diagnosis of dementia was triggered by a change in the CDR scale score from 0.5 to 1.0, and confirmed by physician evaluations and neuropsychological tests. Controls or subjects with AD were not followed over time and their purpose was to determine where subjects with MCI fell in the continuum.

Functional image acquisition. Subjects underwent baseline fMRI scanning at 4.0 T (GE Medical Systems, Milwaukee, WI) during encoding and retrieval of novel and familiar face–name pairs.[13] Anatomic (12.2/5.4/500 [repetition time msec/echo time msec/inversion time msec], flip angle 20°, 256 × 256 matrix, 240-mm field of view) and functional (inverse spiral imaging sequence; 2,500/31 [repetition time msec/echo time msec], flip angle 60°, 64 × 64 matrix, 240-mm field of view) scans were acquired over the same 44 contiguous slice locations in the coronal plane. Three functional scan runs were acquired, lasting 6 minutes 50 seconds, and yielding 164 T2*-weighted volumes each.

Preprocessing. Image preprocessing was performed using statistical parametric mapping software (SPM2; Wellcome Department of Imaging Neuroscience). Images first underwent slice time correction by means of sinc interpolation. Following this, images were motion-corrected and the results screened for excessive movement. Finally, all images were normalized to a standard Montreal Neurological Institute template and smoothed with an 8-mm full width at half maximum Gaussian kernel.

Independent component analysis. ICA is a technique that can decompose an imaging dataset into a number of statistically independent spatial maps, each with its own time course.[14] The sum of these maps, multiplied by their corresponding time courses, approximates the original signal. Group ICA analysis was carried out in the following manner, and is described in detail elsewhere.[15] Preprocessed images were analyzed with software for group ICA (Group ICA of fMRI Toolbox [GIFT], v2.0b, available at http://icatb.sourceforge.net/gift/gift_startup.php) run on MATLAB (version 7.0.4.365 [R14]; Mathworks, Natick, MA). The number of components (maps and corresponding time courses) estimated for each subject was set to 20. In GIFT, principal component analysis was performed first on each subject for dimensionality reduction to decrease computational demands. Data from subjects were then concatenated temporally and a further dimensionality reduction performed on the group. An ICA was performed to estimate the inverse mixing matrix W, where $S = WX$, S being the source matrix of group components and X being the temporally concatenated subject data. Individual subject components were then back-reconstructed from blocks of the group inverse mixing matrix and the individual subject data.

Sorting of components to identify the DMN. To identify which of the 20 group components represented the DMN component, group components were sorted in GIFT through a correlation across voxels with "ref_default_mode," a DMN template supplied in GIFT for DMN identification. The component with the highest spatial correlation was selected. The individual DMN component maps were entered into a z score transform to isolate the pattern of variation in each, $C_z(X) = (C(X) - \mu_c)/\sigma_c$ where $C(X)$ represents the component weighting, μ_c represents the mean and σ_c the SD of component weightings in the map, and $C_z(X)$ represents the z-normalized component weighting.

Calculation of GOF index. A GOF index which reflected the degree to which DMN maps of subjects with AD and subjects with MCI matched those of normal controls was then calculated for each subject. To accomplish this, a normal DMN template was first created in SPM8 using a one-sample t test of

Figure 1 Default mode network (DMN) template

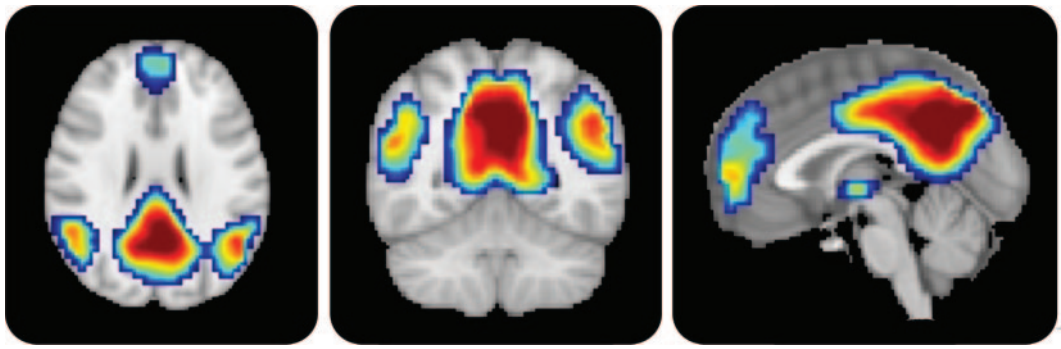

The template mask used for the goodness-of-fit index. Color overlay created from DMN component in normal control subjects based on a one-sample t test corrected for multiple comparisons using a family-wise error correction ($p < 0.05$) and cluster size threshold of 10 voxels. Notice significant clusters of DMN expression in the posterior cingulate/precuneus, ventromedial frontal, and inferior parietal lobule regions.

the normal control subjects' default mode component, thresholded using a family-wise error correction ($p < 0.05$) and cluster extent threshold of 10. Positive values in this template defined a mask which was used to calculate GOF (figure 1). The GOF was calculated in MATLAB as GOF = mean(component[mask]) − mean(component[~mask]), or the mean z score of all voxels within the DMN mask minus the mean z score of all voxels outside the mask (among in-brain voxels), as described previously.[4]

Assessment of gray matter probability in the DMN. To control for the possible confounding effects of differential gray matter volume loss in the DMN, voxel-based morphometry (VBM) was performed on the anatomic images from each subject. Anatomic data were analyzed with FSL-VBM, a voxel-based morphometry style analysis[16,17] carried out with FSL tools.[18] First, structural images were brain-extracted using the Brain Extraction Tool.[19] Next, tissue-type segmentation was carried out using FAST4.[20] The resulting gray matter partial volume images were then aligned to MNI152 standard space using the affine registration tool FLIRT,[21,22] followed by nonlinear registration using FNIRT.[23,24] The resulting images were averaged to create a study-specific template, to which the native gray matter images were then nonlinearly reregistered. The registered partial volume images were then modulated (to correct for local expansion or contraction) by dividing by the Jacobian of the warp field. A mask was created by conjoining the mean GM mask from all subjects with the normal DMN template described in the "Calculation of GOF index" section. This mask was then applied to the partial volume images to obtain a mean DMN gray matter probability for each subject.

Statistical analysis of GOF index. Summary statistics and an analysis of variance with Tukey post hoc testing were used to examine differences in clinical and fMRI variables among the 4 groups (AD, MCI converters, MCI nonconverters, and controls). Logistic regression and multiple regression models were evaluated to examine predictors of cognitive change within subjects with MCI only. Cognitive change (the dependent outcome) was measured as conversion to dementia (categorical) in the logistic regression model, and change from baseline in CDR–sum of boxes (CDR-SB) total score (continuous) in the multiple regression model. Both models included the following independent variables: age, education, baseline Mini-Mental State Examination (MMSE), baseline gray matter volume index, and GOF index. Both models were then modified by substituting the MMSE with the California Verbal Learning Test (CVLT) delayed recall. We performed Pearson correlation coefficients between GOF, CVLT, and fMRI task performance (percent total correct trials inside the scanner). Statistics were computed on MATLAB (Natick, MA).

In addition, to visually depict the DMN in MCI converter and nonconverter groups, we conducted a voxel-wise one-sample t test in SPM8 for each group. Single-subject DMN components from each group were entered into a second level analysis in SPM8 using a threshold of $p < 0.05$, family-wise error corrected, with a cluster extent threshold of 10.

Table 1 Subject characteristics[a]

	NC	MCInc	MCIc	AD	p Value
No.	25	20	11	12	
Age, y	70.8 (4.3)	72.3 (9.2)	76.2 (6.0)	72.0 (5.9)	0.1721
M/F	11/14	7/13	8/3	7/5	0.0821
Education, y	16.0 (2.7)	15.3 (2.2)	14.1 (2.7)	12.7 (2.4)	0.0023
CDR-SB[b]	0.04 (0.14)	0.94 (0.48)	1.45 (0.83)	4.80 (0.59)	<0.0001
CVLT-del[b]	11.2 (2.6)	6.3 (2.1)	3.0 (2.1)	1.3 (1.5)	<0.0001
DMN-GM	0.453 (0.024)	0.441 (0.036)	0.415 (0.028)	0.422 (0.047)	0.0072
MMSE	28.3 (1.4)	27.3 (1.5)	25.8 (1.8)	24.3 (2.3)	<0.0001
fMRI task[b]	0.84 (0.10)	0.80 (0.10)	0.65 (0.11)	0.62 (0.11)	<0.0001

Abbreviations: CDR-SB = Clinical Dementia Rating–sum of boxes score; CVLT-del = California Verbal Learning Test 20-minute delay score; DMN-GM = default mode network gray matter probability; fMRI task performance = percentage correct trials on fMRI task; MCIc = mild cognitive impairment converters; MCInc = mild cognitive impairment nonconverters.

[a] Values are mean (SD).

[b] Denotes statistically significant ($p < 0.05$) difference between MCInc and MCIc.

RESULTS Table 1 summarizes the sample and, as expected, subjects with MCI performed better than subjects with AD and worse than controls on CDR and memory tests. MCI converters tended to be older, less educated, and more impaired in memory than MCI nonconverters, but were not as impaired as subjects with AD. The mean clinical follow-up for

Figure 2 Box whisker plot of goodness-of-fit (GOF) index

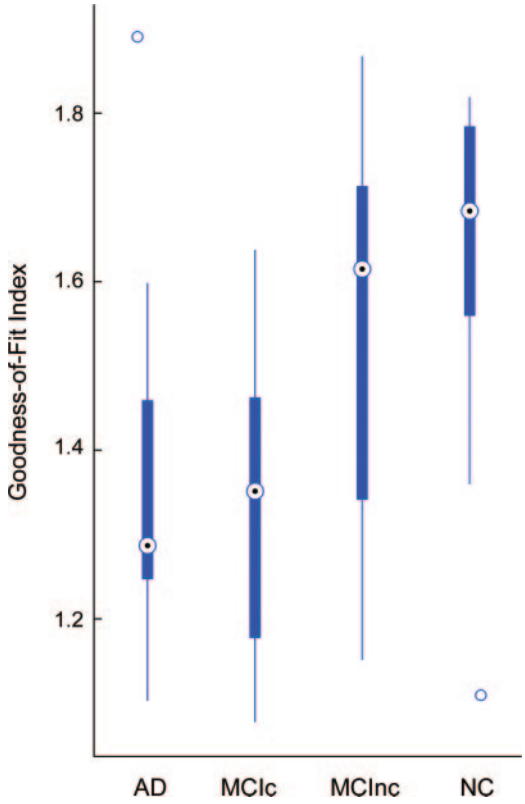

Box whisker plot of GOF index for subjects with Alzheimer disease (AD), mild cognitive impairment converters (MCIc), mild cognitive impairment nonconverters (MCInc), and normal control (NC) groups. Plot depicts the median, interquartile range, and range of values for each group.

subjects with MCI was 2.4 (±0.8) years. Eleven (33%) subjects with MCI converted.

Functional connectivity: GOF index analyses. GOF index differed among the 4 groups ($F = 8.41$, $p < 0.0001$) (figure 2), with the highest values for controls and lowest for subjects with AD. The mean GOF index for the MCI nonconverters was higher than that for MCI converters ($p = 0.02$). Among the MCI group, the GOF index correlated with change from baseline in CDR-SB score ($r = -0.40$, $p = 0.035$). Four models were used to evaluate the effects of clinical, structural imaging, and fMRI variables on cognitive outcomes (conversion to dementia as well as change in CDR-SB) in subjects with MCI at follow-up (table 2). Both GOF index and gray matter index had significant effects on conversion to dementia as well as change in CDR-SB in models that included age, education, and MMSE. In models that included baseline CVLT, GOF index showed a trend to significance with regard to change in CDR-SB. CVLT score was correlated with task performance in the scanner ($p < 0.01$) and GOF index was not a predictor of conversion ($p < 0.09$) when task performance was covaried.

Voxel-wise one-sample *t* tests of DMN expression in the MCI converters and nonconverters revealed significant clusters in the posterior cingulate/precuneus and bilateral inferior parietal lobules in converters and in the posterior cingulate/precuneus and left inferior parietal lobule in nonconverters (figure 3).

DISCUSSION The topographic distribution of the DMN network (posterior cingulate, lateral parietal, medial frontal regions) is similar to that of fibrillar amyloid deposition in patients with AD as determined by in vivo studies using amyloid PET scans, and it has been suggested that overactivity in the DMN in young life may set up a metabolic and physiologic milieu predisposing individuals to amyloid deposition and AD in later life.[2] There is thus great interest in further studies of this network in subjects at risk for AD.

Prior studies have demonstrated a loss of functional connectivity in the DMN in AD and MCI; they have largely been cross-sectional studies designed to identify brain regions in which functional connectivity is altered, to test the diagnostic utility in AD, or to correlate with other biomarkers, such as

Table 2 Results of models examining fMRI connectivity and cognitive decline[a]

	Cognitive outcome tested in models			
Variables in model	**Model 1: conversion to AD**	**Model 2: D CDR-SB**	**Model 3: conversion to AD**	**Model 4: D CDR-SB**
GOF	10.64 (0.025) [20.16 to 1.12]	−3.84 (0.0075) [−1.23 to −6.44]	11.41 (0.17) [28.09 to −5.26]	−2.77 (0.07) [0.17 to −5.70]
DMN-GM	70.75 (0.040) [139.49 to 2.02]	−32.51 (0.0036) [−12.56 to −52.46]	61.62 (0.13) [142.48 to −19.23]	−26.59 (0.01) [−7.60 to −45.59]
Age	0.07 (0.65) [0.37 to −0.23]	−0.01 (0.83) [0.09 to −0.11]	−0.02 (0.95) [0.56 to −0.60]	−0.02 (0.73) [0.08 to −0.11]
Education	0.33 (0.29) [0.96 to −0.30]	−0.13 (0.35) [0.14 to −0.41]	—	—
MMSE	1.16 (0.053) [2.36 to −0.04]	−0.20 (0.30) [0.18 to −0.59]	—	—
CVLT-del	—	—	1.42 (0.075) [3.02 to −0.17]	−0.24 (0.11) [0.05 to −0.52]

Abbreviations: AD = Alzheimer disease; CDR-SB = Clinical Dementia Rating–sum of boxes score; CVLT-del = California Verbal Learning Test delayed recall score; GOF = goodness of fit; DMN-GM = default mode network gray matter probability.
[a] Entries are arranged as follows: parameter value (*p* value) [95% confidence interval].

Figure 3 Mild cognitive impairment nonconverters (MCInc) and mild cognitive impairment converters (MCIc) default mode networks (DMN)

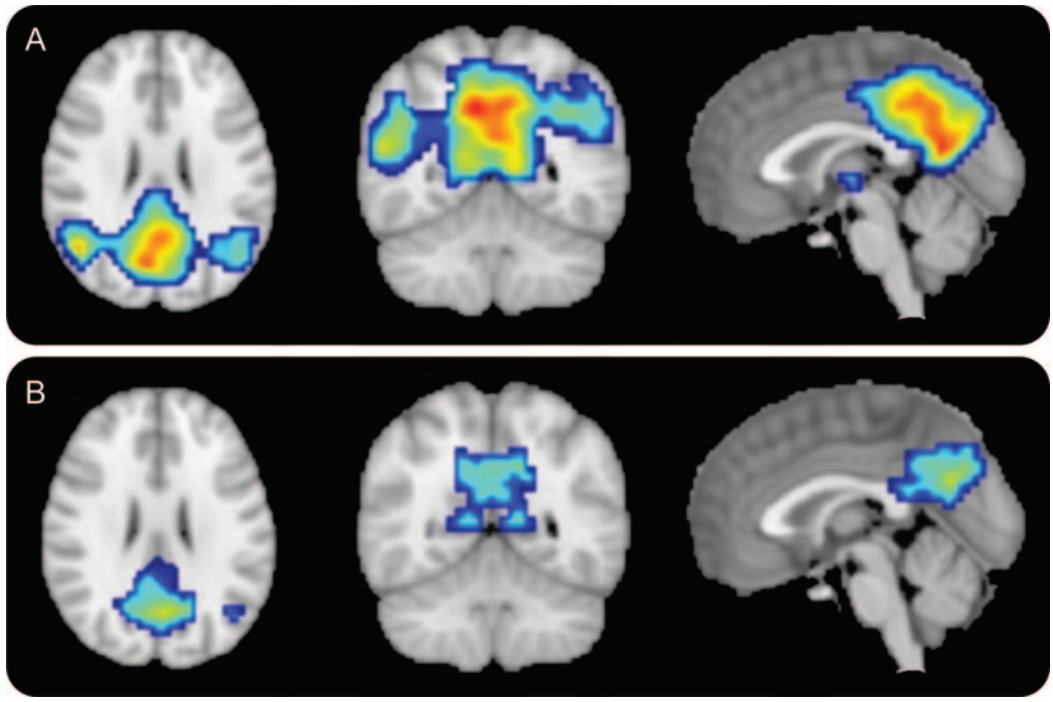

(A) MCInc DMN. (B) MCIc DMN. Cover overlays display the results of one-sample *t* tests in SPM8 corrected for multiple comparisons using a family-wise error correction ($p < 0.05$). Note significant clusters of DMN expression in the posterior cingulate/precuneus and bilateral inferior parietal lobules in the MCInc (A), and in the posterior cingulate/precuneus and left inferior parietal lobule in the MCIc (B).

amyloid PET.[5,8] For example, a prior study[4] proposed the GOF measure in an fMRI study of 13 subjects with AD and 13 elderly controls, finding a sensitivity and specificity of 85% and 77%, for group classification, a range considered clinically relevant by the Working Group on Biomarkers in AD. Our study confirms these prior cross-sectional reports of DMN dysfunction in AD and MCI[12] and extends those with additional new findings. Our study shows that fMRI-measured DMN connectivity GOF indices are in a continuum going from highest integrity in normal elderly to intermediate values in subjects with MCI to lowest in subjects with AD. Further, baseline fMRI DMN indices in MCI were correlated with change from baseline in CDR-SB, a functional global measure widely used in clinical trials. Our models also show a significant relationship between DMN indices and future conversion to AD over a 2- to 3-year follow-up period, above and beyond simple measures routinely used in general practice, such as age and baseline MMSE.

We also examined whether brain atrophy contributed to our fMRI findings by covarying for a VBM-based index of gray matter volume in the DMN. These volumes differed among the 4 groups significantly and volume loss predicted cognitive decline in MCI in some of our models, as expected. However, the effect of fMRI connectivity measures on cognitive decline remained significant after covarying for this gray matter volume index, suggesting that the connectivity differences were independent of regional DMN atrophy. Although we did not measure hippocampal volumes in the current study, there is consensus[25,26] that hippocampal atrophy is an early event in MCI and thus it would be of interest for future studies to examine the relationship between hippocampal atrophy and altered DMN connectivity using a more focused ROI-based connectivity approach to see which comes first and whether the two have a greater predictive value when combined.

Finally, our study found significant correlations between GOF indices and baseline memory performance (recall accuracy) both in clinic and in scanner. This finding is not surprising given that both variables may reflect the underlying relationship between DMN dysfunction and its cognitive manifestations. fMRI indices of DMN connectivity did not have a significant additional predictive value above and beyond baseline neuropsychological measure of delayed recall, which may be reflective of the covariance between these variables. Of note, however, there was a strong trend in both variables, particularly when cognitive decline was treated as a continuous variable (change in CDR-SB score), perhaps a more sensitive

measure than the categorical outcome of conversion. Because our sample size was relatively small, it would be important to test this further in a larger study. Our data show that severity level is on a continuum both cognitively and by DMN connectivity endophenotypes, which in turn is associated with different progression and conversion rates. This is not surprising since it is known that MCI is a heterogeneous group and hence fMRI may offer promise to study brain mechanisms underlying such heterogeneity.

There are technical issues related to our study that merit consideration. The annualized conversion rate in our MCI sample (13%) was in the same range as many prior population studies,[27] suggesting that our sample was similar to other clinical samples.[28] As stated above, the covariance between task performance and disease severity makes it difficult to distinguish the mechanisms underlying fMRI group differences. Our study was performed with generally similar and rigorous methods as that of a prior study,[4] using a data-driven ICA approach. Though the GOF index was calculated in an identical fashion, the prior study used a different task and a template derived from resting state data in young subjects. In both our studies, however, the DMN could be easily extracted in an automated fashion.

Although we used task-related rather than resting-state fMRI data, previous work has shown that the distribution of the major nodes of the DMN determined from resting state or task-related data are quite similar overall.[29,30] This suggests that the main topology of the DMN appears invariant to not only the particulars of a task, but also to whether task-related or resting-state data were acquired, and a robust DMN network can be extracted in a data-driven manner from both resting-state and task-related fMRI data. Of course, resting-state has numerous advantages over task-related fMRI data, including less performance-related variability, less complicated acquisition and standardization, and possibly more effectiveness in identifying functional pathology,[31] and therefore it would be preferable to use resting-state fMRI for clinical biomarker studies, due to simplicity and less performance-related variability. Our sample size and follow-up period were relatively limited. This may explain some of the overlap in GOF index values between nonconverters and subjects with AD and it is possible that a longer follow-up period might have yielded cleared separation of subjects at an individual level. Hence our data should be viewed as hypothesis generating rather than confirmatory, and a larger study with longer follow-up could be designed based on our findings to test potential prognostic utility. Our measure of connectivity (GOF index), while data-driven, is not necessarily the only approach and, as stated previously, region of interest–based connectivity approaches may yield complimentary insights.

We focused just on the DMN network, although it is known that there are multiple networks in the brain that might be related to cognition and AD. In the future, one may consider supplementing DMN connectivity analyses with other resting-state or task-related networks, an approach which has been shown to improve classification of neuropsychiatric disease and may optimize future applications of functional connectivity to prediction of cognitive outcome in MCI.[32] Our findings may also have implications for the use of DMN indices as a biomarker in therapeutic trials.[33]

DISCLOSURE

Dr. Petrella has served on a scientific advisory board for Janssen; has received research support from Avid Radiopharmaceuticals, Inc., Pfizer Inc, Eisai Inc., and the NIH/NIA; and has served as an expert witness in a medico-legal case. Mr. Sheldon has received salary support from Avid Radiopharmaceuticals, Inc. Dr. Prince has received research support from Pfizer Inc. Dr. Calhoun has received research support from the NIH, the National Science Foundation, and the US Department of Energy; has served as a consultant in medico-legal cases; has performed grant reviews for the NIH; has received support for fMRI training courses; and has generated books or book chapters for publishers of various texts. Dr. Doraiswamy has served on scientific advisory boards for AARP, Dana Foundation, Forest Laboratories, Inc., Medivation, Inc., Bristol-Myers Squibb, Accera, Inc., Avid Radiopharmaceuticals, Inc., Sonexa Therapeutics, Inc., Bayer Schering Pharma, the Alzheimer's Foundation, and the Alzheimer's Association; has received funding for travel or speaker honoraria from Otsuka Pharmaceutical Co., Ltd., Bristol-Myers Squibb, the Alzheimer's Association, the NIH, Accera, Inc., Neuroptix Corporation, Neuronetrix, Inc., Medivation, Inc., GE Healthcare, TauRx Pharmaceuticals, Lundbeck Inc., and Forest Laboratories, Inc.; serves on the editorial board of *Pharmacotherapy*; is coinventor on a patent assigned to Duke University re: cholinesterase inhibitors for treating disorders in children; receives publishing royalties for *The Alzheimer's Action Plan* (St. Martin's Press, 2008) and from AARP Magazine; has served as a consultant for Bayer Schering Pharma, Rutgers University, and the NIH (grant reviews); serves on speakers' bureaus for Forest Laboratories, Inc. and Merck Serono; owns stock in Sonexa Therapeutics, Inc.; and receives research support (to Duke University) from Avid Radiopharmaceuticals, Inc., Elan Corporation, Eli Lilly and Company, Neuronetrix, Inc., Medivation, Inc., Bristol-Myers Squibb, Ono Pharmaceutical Co. Ltd., sanofi-aventis, Novartis, GlaxoSmithKline, Forest Laboratories, Inc. Eisai Inc., the NIH (NIA/NIMH/NINDS), NARSAD, American Federation for Aging Research, and the Alzheimer's Drug Discovery Foundation.

Received August 10, 2010. Accepted in final form September 20, 2010.

REFERENCES

1. Buckner RL, Andrews-Hanna JR, Schacter DL. The brain's default network. Ann NY Acad Sci 2008;1124:1–38.
2. Buckner RL, Snyder AZ, Shannon BJ, et al. Molecular, structural, and functional characterization of Alzheimer's disease: evidence for a relationship between default activity, amyloid, and memory. J Neurosci 2005;25:7709–7717.
3. Bai F, Watson DR, Yu H, Shi Y, Yuan Y, Zhang Z. Abnormal resting-state functional connectivity of posterior cingulate cortex in amnestic type mild cognitive impairment. Brain Res 2009;1302:167–174.

4. Greicius MD, Srivastava G, Reiss AL, Menon V. Default-mode network activity distinguishes Alzheimer's disease from healthy aging: evidence from functional MRI. Proc Natl Acad Sci USA 2004;101:4637–4642.
5. Hedden T, Van Dijk KR, Becker JA, et al. Disruption of functional connectivity in clinically normal older adults harboring amyloid burden. J Neurosci 2009;29:12686–12694.
6. Rombouts SA, Barkhof F, Goekoop R, Stam CJ, Scheltens P. Altered resting state networks in mild cognitive impairment and mild Alzheimer's disease: an fMRI study. Hum Brain Mapp 2005;26:231–239.
7. Sorg C, Riedl V, Muhlau M, et al. Selective changes of resting-state networks in individuals at risk for Alzheimer's disease. Proc Natl Acad Sci USA 2007;104:18760–18765.
8. Sheline YI, Raichle ME, Snyder AZ, et al. Amyloid plaques disrupt resting state default mode network connectivity in cognitively normal elderly. Biol Psychiatry 2010;67:584–587.
9. Sperling RA, Laviolette PS, O'Keefe K, et al. Amyloid deposition is associated with impaired default network function in older persons without dementia. Neuron 2009;63:178–188.
10. Van Dijk KRA, Hedden T, Venkataraman A, Evans KC, Lazar SW, Buckner RL. Intrinsic functional connectivity as a tool for human connectomics: theory, properties, and optimization. J Neurophysiol 2010;103:297–321.
11. Friston K, Buchel C. Functional connectivity: eigenimages and multivariate analyses. In: Statistical Parametric Mapping: The Analysis of Functional Brain Images. Academic Press; 2006:492–507.
12. Liu Y, Wang K, Yu C, et al. Regional homogeneity, functional connectivity and imaging markers of Alzheimer's disease: a review of resting-state fMRI studies. Neuropsychologia 2008;46:1648–1656.
13. Petrella JR, Krishnan S, Slavin MJ, Tran TT, Murty L, Doraiswamy PM. Mild cognitive impairment: evaluation with 4-T functional MR imaging. Radiology 2006;240:177–186.
14. McKeown MJ, Makeig S, Brown GG, et al. Analysis of fMRI data by blind separation into independent spatial components. Hum Brain Mapp 1998;6:160–188.
15. Calhoun VD, Adali T, Pearlson GD, Pekar JJ. A method for making group inferences from functional MRI data using independent component analysis [erratum in 2002; 16:131]. Hum Brain Mapp 2001;14:140–151.
16. Ashburner J, Friston KJ. Voxel-based morphometry: the methods. Neuroimage 2000;11:805–821.
17. Good CD, Johnsrude IS, Ashburner J, Henson RNA, Friston KJ, Frackowiak RSJ. A voxel-based morphometric study of ageing in 465 normal adult human brains. Neuroimage 2001;14:21–36.
18. Smith SM, Jenkinson M, Woolrich MW, et al. Advances in functional and structural MR image analysis and implementation as FSL. Neuroimage 2004;23:S208–S219.
19. Smith S. Fast robust automated brain extraction. Hum Brain Mapp 2002;17:143–155.
20. Zhang Y, Brady M, Smith S. Segmentation of brain MR images through a hidden Markov random field model and the expectation-maximization algorithm. IEEE Trans Med Imaging 2001;20:45–57.
21. Jenkinson M, Smith S. A global optimisation method for robust affine registration of brain images. Med Image Anal 2001;5:143–156.
22. Jenkinson M, Bannister P, Brady M, Smith S. Improved optimization for the robust and accurate linear registration and motion correction of brain images. Neuroimage 2002;17:825–841.
23. Andersson JLR, Jenkinson M, Smith S. Non-linear optimisation. FMRIB technical report TR07JA1 from www.fmrib.ox.ac.uk/analysis/techrep. Accessed June 1, 2010.
24. Andersson JLR, Jenkinson M, Smith S. Non-linear registration, aka Spatial normalisation. FMRIB technical report TR07JA2 from www.fmrib.ox.ac.uk/analysis/techrep. Accessed June 1, 2010.
25. Vemuri P, Wiste HJ, Weigand SD, et al. Serial MRI and CSF biomarkers in normal aging, MCI, and AD. Neurology 2010;75:143–151.
26. Jack CR Jr, Bernstein MA, Borowski BJ, et al. Update on the magnetic resonance imaging core of the Alzheimer's Disease Neuroimaging Initiative. Alzheimer Dementia 2010;6:212–220.
27. Petersen RC. Mild cognitive impairment clinical trials. Nat Rev Drug Discov 2003;2:646–653.
28. Petersen RC, Thomas RG, Grundman M, et al. Vitamin E and donepezil for the treatment of mild cognitive impairment. N Engl J Med 2005;352:2379–2388.
29. Calhoun VD, Kiehl KA, Pearlson GD. Modulation of temporally coherent brain networks estimated using ICA at rest and during cognitive tasks. Hum Brain Mapp 2008;29:828–838.
30. Buckner RL, Sepulcre J, Talukdar T, et al. Cortical hubs revealed by intrinsic functional connectivity: mapping, assessment of stability, and relation to Alzheimer's disease. J Neurosci 2009;29:1860–1873.
31. Fleisher AS, Sherzai A, Taylor C, Langbaum JB, Chen K, Buxton RB. Resting-state BOLD networks versus task-associated functional MRI for distinguishing Alzheimer's disease risk groups. NeuroImage 2009;47:1678–1690.
32. Calhoun VD, Maciejewski PK, Pearlson GD, Kiehl KA. Temporal lobe and "default" hemodynamic brain modes discriminate between schizophrenia and bipolar disorder. Hum Brain Mapp 2008;29:1265–1275.
33. Laxton AW, Tang-Wai DF, McAndrews MP, et al. A phase I trial of deep brain stimulation of memory circuits in Alzheimer's disease. Ann Neurol Epub 2010.